Preclinical Study of Ublituximab, a Glycoengineered Anti-Human CD20 Antibody, in Murine Models of Primary Cerebral and Intraocular B-Cell Lymphomas

Rym Ben Abdelwahed,[1–4] Sabrina Donnou,[1–3] Hanane Ouakrim,[1–3] Lucile Crozet,[1–3] Jérémie Cosette,[1–3] Alexandra Jacquet,[5] Isabel Tourais,[5] Bénédicte Fournès,[5] Mélanie Gillard Bocquet,[1–3] Amine Miloudi,[1–3] Valérie Touitou,[1–3,6] Cécile Daussy,[1–3] Marie-Christine Naud,[1–3] Wolf Herman Fridman,[1–3] Catherine Sautès-Fridman,[1–3] Rémi Urbain,[5] and Sylvain Fisson[1–3,7–9]

[1]Institut National de la Santé et de la Recherche Médicale (INSERM), UMRS872, Centre de Recherche des Cordeliers, Paris, France
[2]Université Pierre et Marie Curie-Paris 6, UMRS 872, Paris, France
[3]Université Paris Descartes, UMRS 872, Paris, France
[4]Université de Monastir, Monastir, Tunisie
[5]Laboratoire français du Fractionnement et des Biotechnologies (LFB), Les Ulis, France
[6]Département d'Ophtalmologie, Hôpital de la Pitié-Salpêtrière, Paris, France
[7]Généthon, Evry, France
[8]INSERM, U951, Evry, France
[9]Université d'Evry Val d'Essonne, UMRS 951, Evry, France

Correspondence: Sylvain Fisson, Généthon, INSERM UMRS 951, 1 bis rue de l'Internationale, Evry F-91002, France; sylvain.fisson@univ-evry.fr.

RBA and SD contributed equally to the work presented here and should therefore be regarded as equivalent authors.

Submitted: June 1, 2012
Accepted: April 16, 2013

Citation: Abdelwahed RB, Donnou S, Ouakrim H, et al. Preclinical study of ublituximab, a glycoengineered anti-human CD20 antibody, in murine models of primary cerebral and intraocular B-cell lymphomas. *Invest Ophthalmol Vis Sci*. 2013;54:3657–3665. DOI:10.1167/iovs.12-10316

Purpose. Primary cerebral lymphoma (PCL) and primary intraocular lymphoma (PIOL) belong to the systemic diffuse large B-cell lymphoma family and are characterized by the presence of $CD20^+$ lymphoma B cells in the brain or the eye. These highly aggressive malignancies have a poor prognosis and no specific therapy. The presence of effector immune cells in the damaged brain and vitreous suggests that treatment with anti-human CD20 (hCD20) monoclonal antibodies might be effective. We developed murine models of PCL and PIOL to assess the intracerebral and intraocular antitumor effect of ublituximab, a promising glycoengineered anti-hCD20 mAb with a high affinity for FcγRIIIa (CD16) receptors.

Methods. The murine lymphoma B-cell line A20.IIA-GFP-hCD20 ($H\text{-}2^d$) was injected into the right cerebral striatum or the vitreous of immunocompetent adult BALB/c mice ($H\text{-}2^d$). Four to 7 days later, ublituximab was injected intracerebrally or intravitreously into the tumor site. Rituximab was the reference compound. Survival was monitored for injected mice; histopathological and flow cytometric analyses were performed to study tumor growth and T-cell infiltration.

Results. Single doses of ublituximab, injected intracerebrally or intravitreously, had a marked antitumor effect, more pronounced than that obtained with the same dose of rituximab in these conditions. The reduction in tumor cells was correlated with an increased proportion of $CD8^+$ T cells. This efficacy was observed only against lymphoma B cells expressing hCD20.

Conclusions. These in vivo results confirm the potential of the glycoengineered anti-hCD20 mAb ublituximab as an innovative therapeutic approach to treat primary central nervous system lymphoma and other B-cell lymphomas.

Keywords: glycoengineered monoclonal antibody, human CD20, primary intracerebral B cell lymphoma (PCL), primary intraocular B cell lymphoma (PIOL), primary vitreoretinal lymphoma (PVRL), ublituximab

Primary central nervous system lymphoma (PCNSL) is a form of extranodal high-grade non-Hodgkin B-cell neoplasms[1] that can originate in the brain, leptomeninges, spinal cord, or eyes,[2,3] typically remains confined to the CNS, and rarely spreads outside the nervous system. PCNSL accounts for 1% to 4% of primary brain tumors.[4]

Primary cerebral lymphoma (PCL) and primary intraocular lymphoma (PIOL, also called primary vitreoretinal lymphoma, PVRL) are closely related subsets of PCNSL that reach these two immunoprivileged sites.[5] PCL is a tumor of the brain parenchyma. Tumor cells are usually found around blood vessels and PCL can develop as a uni- or multifocal tumor. PIOL is an aggressive malignancy in which lymphoma cells spread in the retina, vitreous, or optic nerve. It may be limited to the eye, but may also include CNS involvement. Approximately 95% of PCLs and 98% of PIOLs express CD19 and CD20.[4] The

prognosis of immunocompetent patients diagnosed with PCNSL has improved over the past decade with methotrexate administration and cranial radiotherapy.[6] This first-line therapy fails in 35% to 60% of cases, however, and the prognosis for patients with PCL or PIOL or both remains poor, with a median overall survival of only 33 to 40 months.[7] Because these tumor cells express CD20, a well-characterized antigen, immunotherapy has become a new area of active research.

mAbs have already been used successfully to treat tumors: trastuzumab for Her/Neu-positive breast cancer,[8] and rituximab, a mouse-human chimeric mAb that targets human CD20 (hCD20), for CD20-positive non-Hodgkin lymphomas.[9] Studies have shown it is active against central nervous system (CNS) lymphoma after both intravenous[10] and intraventricular[6] injection and have thus demonstrated the interest of such a strategy for brain tumors. Clinical response was nonetheless limited, which might be explained by rituximab's inadequate engagement of antibody-dependent cell-mediated cytotoxicity (ADCC) or the limited availability of the complement system in the central nervous system.[11] Ublituximab is a promising glycoengineered chimeric anti-hCD20 mAb that has a high affinity for FcγRIIIa (CD16) receptors and therefore greater ADCC activity than rituximab.[12,13]

In this study, we sought to evaluate the efficacy of ublituximab in murine models of PCNSL. B-lymphoma cells were stably transfected with the human CD20 antigen. After implantation in the brain (PCL model) or the eye (PIOL model), we evaluated the therapeutic potential of ublituximab administered directly into the tumor. In these conditions, these injections into the brain and vitreous body resulted in more effective regression of the induced tumor than with rituximab.

Materials and Methods

Mice

Female BALB/c mice (H-2^d) were obtained from Charles River Laboratories (L'Arbresle, France) and used between 6 and 8 weeks of age. They were provided with sterile food and water ad libitum and kept on a 12-hour light-dark cycle. All mice were manipulated according to the ARVO Statement for the Use of Animals in Ophthalmic and Vision Research, the European Union guidelines, and with the approval of the local research ethics committee (Charles Darwin Ethics Committee in Animal Experiment, Paris, France; Permit Number: p3/2009/004).

Cells

A20.IIA (also called IIA1.6) is an FcγR-negative clone originating from the A20-2J B-cell lymphoma line.[14] A20.IIA cells were transfected by an electroporation system with the green fluorescent protein (GFP) gene or with a gene containing a fusion protein of GFP and the human CD20 (hCD20, cloned from the Raji cell line). These cells, hereafter referred to as A20.IIA-GFP or A20.IIA-GFP-hCD20 cells (Supplementary Fig. S1A), were maintained at 37°C, 5% CO_2 in complete Roswell Park Memorial Institute (RPMI) 1640 Medium GlutaMAX Plus (RPMI; Gibco-Invitrogen, Saint Aubin, France) supplemented with 10% fetal calf serum (FCS; PAA laboratories, Cölbe, Germany); 100 U/mL penicillin and 100 μg/mL streptomycin (both from Eurobio, Courtaboeuf, France); 10 mM sodium pyruvate (Gibco-Invitrogen); 50 μM 2-mercaptoethanol (Gibco-Invitrogen); and 0.5 mg/mL neomycin (G418; Gibco-Invitrogen). To obtain the A20.IIA- GFP-hCD20- luc2 cell line, A20.IIA-GFP-hCD20 cells were transfected with pGL4.50[luc2/CMV/hygro] (Promega, Madison, WI), in a commercial device (Amaxa Nucleofector II; Lonza, Basel, Switzerland) and were cultured in 1 mg/mL neomycin and 0.75 mg/mL hygromycinB (Gibco-Invitrogen) medium.

Tumor Implantation

Mice were first anesthetized by intraperitoneal injection of a mixture containing 120 mg/kg of ketamine (Virbac, Carros, France) and 6 mg/kg of xylazine (Rompun 2%; Bayer Healthcare, Loos, France). Anesthetized mice were immobilized on a stereotaxic frame (David Kopf Instruments, Tujunga, CA) for the intracerebral tumor implantation. Tumor cells (5×10^4 in a final volume of 2 μL) were injected into the specific cerebral location (right striatum), located 2 mm to the right of the medial suture and 0.4 mm in front of the bregma, through a Hamilton syringe attached to a penetrating depth controller. The penetrating depth of the syringe was 2.5 mm from the surface of the brain. Each injection delivered the solution slowly, and the syringe was held in place for an additional minute to reduce backfilling of tumor cells. The same procedure was used for control mice injected with 1× phosphate-buffered saline (pH7.4; PBS). For the intravitreal tumor implantation, we used a 32-gauge needle attached to a syringe to inject 10^4 cells in a final volume of 2 μL into the vitreous under a dissecting microscope. Eye drops (Lacrinorm 2%; Bausch + Lomb, Montpellier, France) were instilled after intravitreal injection.

Description of Ublituximab

Ublituximab is a chimeric mAb produced by LFB Biotechnologies (Les Ulis, France) and has previously been described as EMAB-6.[12] Briefly, this chimeric mAb was generated from a mouse IgG2a kappa type I light chain, anti-human CD20 mAb named CAT-13.6E12 (DSMZ, Braunschweig, Germany). IGKV and IGHV were cloned into expression vectors containing a human kappa light chain constant region (IGKC) or a human heavy chain constant gamma 1 region (IGHG1), respectively. Compared with rituximab, this antibody has a lower fucose content in its Fc region. Apoptosis and complement-dependent cytotoxicity (CDC) were almost comparable with that induced by rituximab, whereas FcγRIIIA binding and FcγRIIIA-dependent effector functions were highly improved.

Anti-hCD20 Injections and Clinical Follow-Up

The brain tumors were treated by a single therapeutic injection made intracranially 7 days after the tumor inoculation. Each mouse was treated by PBS (control groups), or by 1, 5, or 20 μg of ublituximab, or by 20 μg of rituximab. Survival was monitored daily.

In the PIOL model, the therapeutic mAbs were injected directly into the eye 4 or 7 days after tumor inoculation. Ublituximab was used at doses of 1, 4, or 20 μg, and rituximab at 20 μg. Control groups received 2 μL of PBS. All doses of ublituximab and rituximab were administered intracranially or intravitreously in a final volume of 2 μL.

In Vivo Tumor Growth Assay

A20.IIA stable cell line (1×10^4) cells expressing luciferase (luc2 gene) were injected via the intravitreal route into immunocompetent 7-week-old BALB/c mice. Tumor formation and metastases were analyzed every week for 8 weeks. Mice were injected with 150 mg/kg of D-luciferin potassium salt (Interchim, San Pedro, CA) via the intraperitoneal route and underwent imaging within 15 minutes afterwards by a commercial imaging system (IVIS LUMINA2; Caliper LS, Hopkinton, MA). The exposure time was set to optimize the

Investigative Ophthalmology & Visual Science

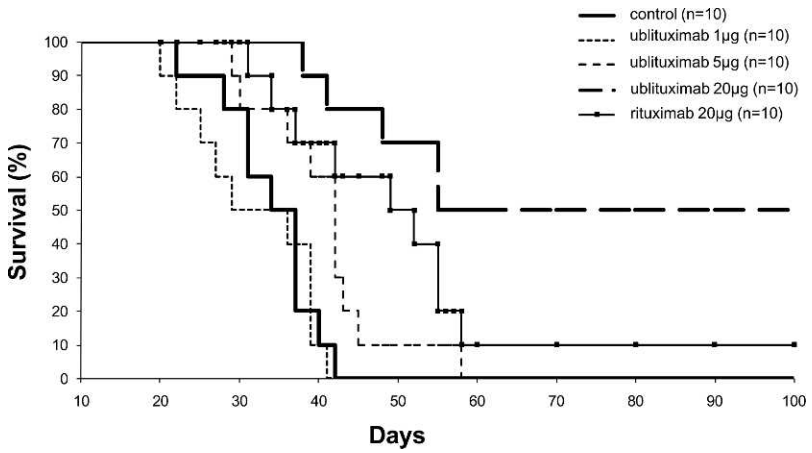

FIGURE 1. Analysis of the dose-response antitumor effect of anti-hCD20 mAb on the murine PCL model and comparison with rituximab. Kaplan-Meier survival analysis after brain inoculation with A20.IIA-GFP-hCD20 cells. On day 7 after this inoculation, the mice were treated intracerebrally with 1 µg/2 µL or 5 µg/2 µL or 20 µg/2 µL anti-hCD20 ublituximab, and compared with a control group treated with PBS 1× and another group treated with 20 µg/2 µL rituximab. Survival was followed daily, and results obtained from two independent experiments were pooled. Statistical test: Log-rank between the PBS 1× control group and group treated with: 5 µg/2 µL ublituximab ($P = 0.024$); 20 µg/µL ublituximab ($P < 0.001$); 20 µg/µL rituximab ($P = 0.028$).

signal and obtain the best signal over noise ratio. The unit of the bioluminescence signal is photons per second. Images were taken of the front and of the back of each mouse. A region of interest (RoI) was drawn around the mice to insure inclusion of potential metastases. The total influx of photons used to quantify the tumor growth is the sum of the influx of photons gathered from the front and back of the mouse.

Brain and Ocular Cell Isolation

The tumor-injected brain or eye of each mouse was harvested and minced with surgical scissors; incubated for 30 minutes in RPMI containing 0.1 mg/mL DNAse I (Roche Diagnostics, Meylan, France) and 1.67 Wûnch U/mL Liberase (Roche); and filtered through a 70-µm membrane (BD Falcon; BD Biosciences, San Jose, CA). A Percoll gradient was used to separate live mononuclear cells from myelin.

Flow Cytometric Analyses

After 20 minutes of Fc receptor saturation with 10 µg/mL anti-CD16/CD32 mAb (clone 2.4.G2), cells were incubated for 20 minutes with the following mAbs: rat IgG2a anti-CD19/APC, or rat IgG2a anti-CD8/AF700, or the corresponding isotypic mAb controls (all from BD Biosciences). The living cells were defined with side scatter and forward scatter, after exclusion of autofluorescent cells. Cell phenotypes were analyzed with the LSRII cytometer and commercial analytical software (BD FACSDiva; BD Biosciences).

Histopathological Analyses

After sacrifice at day 21, eyes and brain were collected, postfixed in 4% paraformaldehyde (PFA) for 4 hours (eyes) or overnight (brain), PFA containing 5% sucrose for 2 hours, and PFA containing 15% sucrose overnight. After alcohol and toluene baths, serial sections (8 µm) were performed by a microtome (Leica RM 2145; Leica Microsystems GmBH, Wetzlar, Germany) from paraffin-embedded preparations and stained with hematoxylin-eosin-safran for eye sections or with hematoxylin-phloxine-safran for brain sections. Images were collected with commercial equipment and software (Nikon Eclipse E600W, Nikon Instruments, Champigny sur Marne, France; Cartograph; Microvision Instruments, Evry, France).

Statistical Analysis

Comparisons used Mann-Whitney test and Kaplan-Meier curves, performed with commercial graphing software (GraphPad Prism; GraphPad Software, La Jolla, CA). Statistical significance was defined by P values less than 0.05.

RESULTS

Anti-hcd20 Ublituximab Has a More Sustained and Better Antitumor Effect Than Rituximab on Primary Cerebral Lymphoma In Vivo

To evaluate the efficacy of the anti-human CD20 ublituximab mAb in our PCL murine model, A20.IIA lymphoma B cells transfected with GFP and hCD20 (A20.IIA-GFP-hCD20) were injected stereotactically into the right striatum of adult syngeneic BALB/c mice. Seven days later, these mice received 1 µg, 5 µg, or 20 µg of anti-hCD20 ublituximab, or 20 µg of rituximab, or PBS (the control group). The PBS 1× control group differed significantly from all ublituximab-treated groups, except the group receiving the smallest dose (1 µg anti-hCD20 ublituximab; Fig. 1), which indicates a dose-effect relation. Specifically, it differed from ublituximab at 20 µg ($P < 0.001$) and at 5 µg ($P = 0.024$). Interestingly, half of the mice treated with 20 µg of this new mAb rejected their tumors. An irrelevant glycoengineered mAb of the same isotype as ublituximab was used as a positive control, and this control group did not differ significantly from the PBS negative control group (Supplementary Fig. S1B).

Because results from clinical use of rituximab have been encouraging, it was chosen in this study as the reference for ublituximab. Clinical manifestations in our PCL model appeared the week before death and were characterized by weight loss, postural prostration, and/or spiky hairs. Surviving mice did not develop any clinical signs. Results in Figure 1 show that when injected at the same dose of 20 µg, ublituximab had a stronger effect on lymphoma cells than rituximab ($P = 0.0028$). Moreover, the overall survival of these two treatment groups was clearly different: 50% survival (5/10) with ublituximab versus 10% survival (1/10) with rituximab. These results were confirmed by flow cytometry analyses showing the percentage of GFP^+ $CD19^+$ tumor cells among live

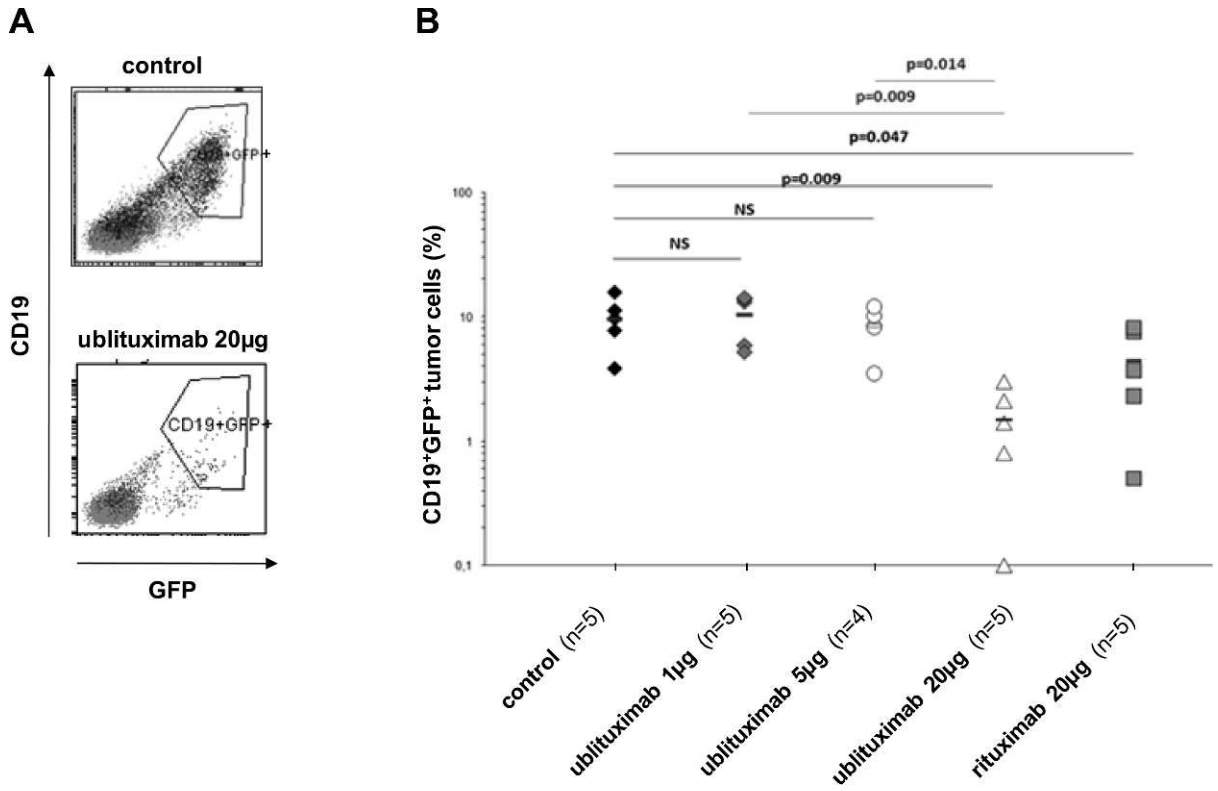

Figure 2. Analysis of the effect of anti-hCD20 ublituximab on tumor growth. (**A**) Flow cytometric analysis at day 21 of GFP$^+$ CD19$^+$ tumor cells in the brain treated with 2 µL PBS (control; *top panel*) or 20 µg anti-hCD20 ublituximab (*lower panel*). (**B**) Percentage of CD19$^+$ GFP$^+$ tumor cells among live mononuclear cells, as determined by flow cytometry, in the brain of mice treated with 1 µg/2 µL, 5 µg/2 µL, or 20 µg/2 µL anti-hCD20 ublituximab, compared with the PBS control group and the group treated with 20 µg/2 µL rituximab ($n = 5$). Statistical test: Mann-Whitney; NS, not significant.

mononuclear cells 14 days after treatment (Fig. 2). As expected, the antitumor effect of ublituximab at 20 µg was very significant ($P = 0.009$) at the cellular level, compared with the PBS 1× control group. The difference between the lower doses tested (1 µg and 5 µg) and the control did not reach statistical significance at this time point. Flow cytometric analyses of the percentage of CD19$^+$ GFP$^+$ tumor cells in the brain also confirmed the therapeutic efficacy of rituximab at 20 µg, but showed that it was weaker ($P = 0.047$) than that of ublituximab. Moreover, the decrease of the percentage of tumor cells was correlated with an increase in the number (Fig. 3) and percentage (Supplementary Fig. S2A) of CD8$^+$ T cells in the brains of treated mice.

The bioluminescence imaging system allowed us to assess total photon influx, which is representative of the tumor burden of the whole mouse, and to compare it between ublituximab-treated mice and PBS-injected (control) mice. On day 10 (i.e. 3 days after treatment), the intracerebral tumor was no longer detectable in the treatment group (Fig. 4A). This was confirmed by histological analysis showing that no tumor mass could be detectable at day 21 in ublituximab-treated mice in contrast with control mice (Fig. 4B). At day 29, some control mice had cervical lymph node metastasis, with 1.6×10^6 ph/s/cm^2/sr luminescence signal (Fig. 4A, RoI 1 in the upper panel), which is a 100 times higher than the signal from an area expected to be negative (Fig. 4A, RoI 2 in the upper panel). The ublituximab-treated representative mouse had 4.4×10^3 ph/s/cm^2/sr in the right cervical lymph node, a photon influx one-thousandth less intense than in the control mouse.

To rule out the possibility of a nonspecific effect of ublituximab, animals were implanted with tumors that did (A20.IIA-GFP-hCD20) or did not (A20.IIA-GFP) express the human CD20 antigen and were treated with 20 µg of the therapeutic mAb. As expected, mice without treatment all died after 37 days regardless of the tumor (Fig. 5). Ublituximab was

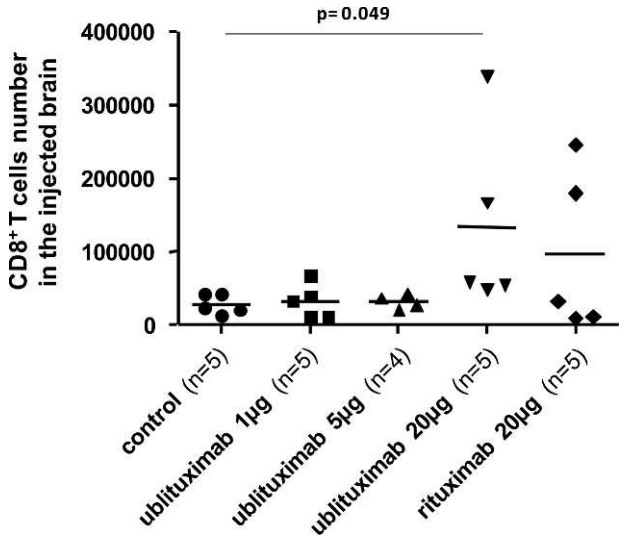

Figure 3. Effect of an intracerebral injection of anti-hCD20 mAb on the absolute number of CD8$^+$ cells in the brain. Absolute number of CD8$^+$ T-cells was analyzed by flow cytometry in the brain of mice treated with 1 µg/2 µL, 5 µg/2 µL, or 20 µg/2 µL anti-hCD20 ublituximab, in comparison with the PBS control group and the group treated with 20 µg/2 µL rituximab. Statistical test: Mann-Whitney.

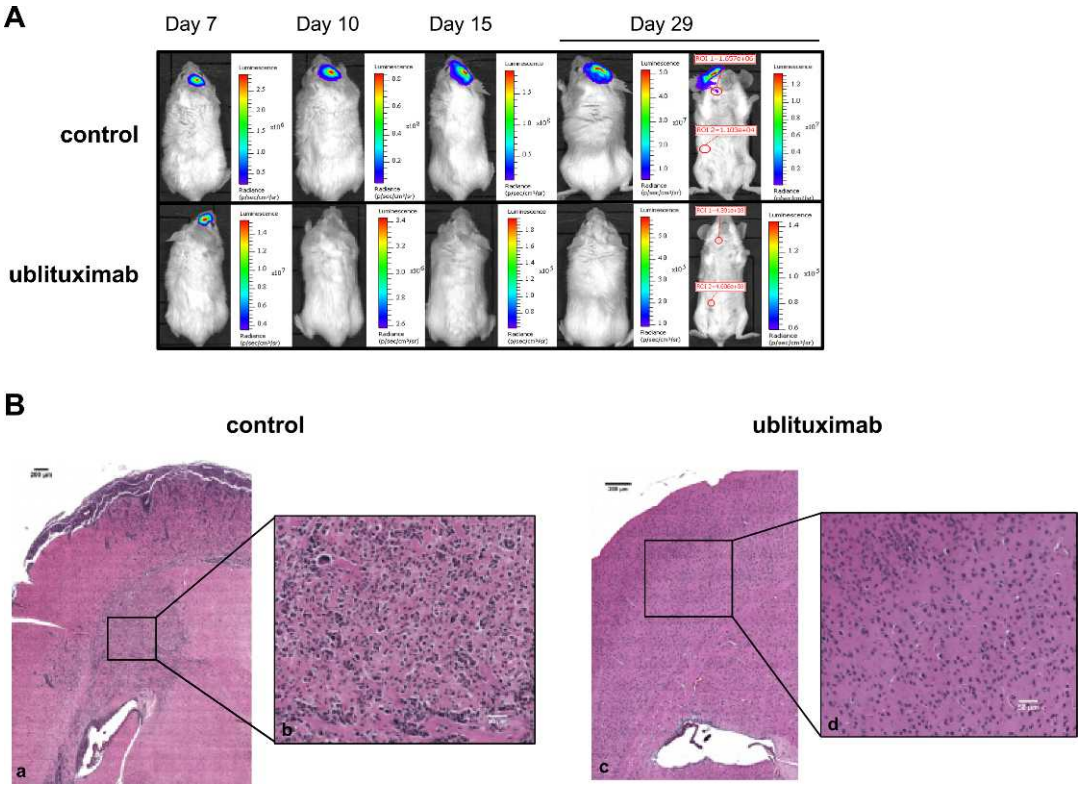

FIGURE 4. Representative bioluminescence images and histopathological analysis comparing ublituximab treatment with PBS injection in PCL murine model. (**A**) Representative bioluminescence images of PBS control PCL mice (*upper panel*) and ublituximab-treated PCL mice (*lower panel*). The mice were injected with 5.10^4 A20.IIA-GFP-hCD20-luc2 cells on day 0 via the intracranial route. The ublituximab treatments were administered in situ on day 7. The figure shows a view of the front of mouse on day 29, with a metastasis detected in the right cervical lymph node. (**B**) Representative histological aspect of PBS control PCL mice (*left panels*) and ublituximab-treated PCL mice (*right panels*). The mice were injected with 5.10^4 A20.IIA-GFP-hCD20-luc2 cells on day 0 via the intrastriatal route. The ublituximab treatments were administered in situ at day 7 and sacrificed at day 21. (**a**, **c**) Magnification ×20 and *bars* represent 200 μm. (**b**, **d**) Magnification ×40 and *bars* represent 50 μm.

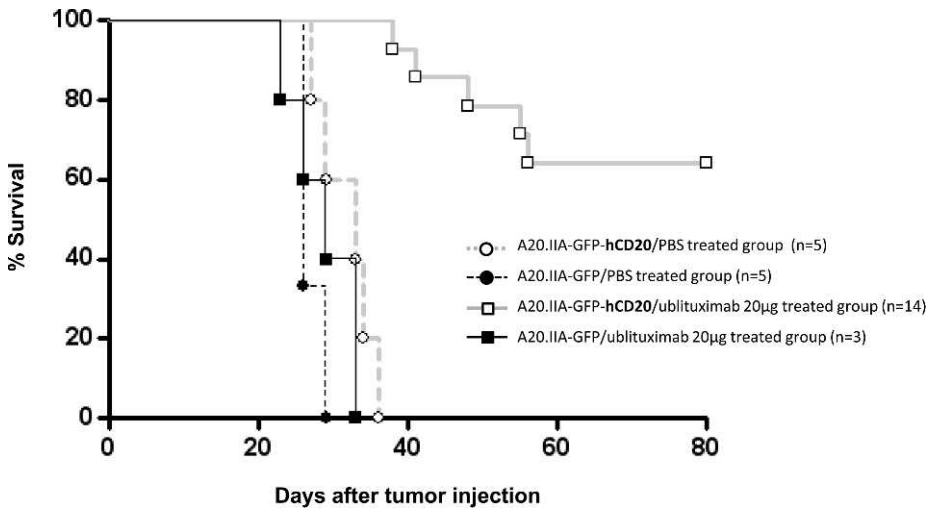

FIGURE 5. Analysis of the anti-hCD20 specificity of ublituximab in the murine PCL model. Kaplan-Meier survival analysis after brain inoculation with A20.IIA-GFP-hCD20 or A20.IIA-GFP tumor cells. On day 7 after this inoculation, the mice received an intracerebral injection of 20 μg/2 μL anti-hCD20 ublituximab, and were compared with the control group receiving an injection of PBS. Survival was followed daily. Statistical test: Log rank between the group injected with A20.IIA-GFP-hCD20 tumor cells and treated with ublituximab 20 μg and the group injected with A20.IIA-GFP tumor cells and treated with ublituximab 20 μg ($P < 0.0001$) and between the group injected with A20.IIA-GFP-hCD20 tumor cells and treated with PBS 1× (control group) and the group injected with A20.IIA-GFP tumor cells and treated with ublituximab 20 μg ($P < 0.0001$). Moreover a significant difference ($P < 0.0001$) was found between the group injected with A20.IIA-GFP-hCD20 tumor cells and treated with PBS 1× (control group) and the group injected with A20.IIA-GFP-hCD20 tumor cells and treated intracerebrally with ublituximab 20 μg.

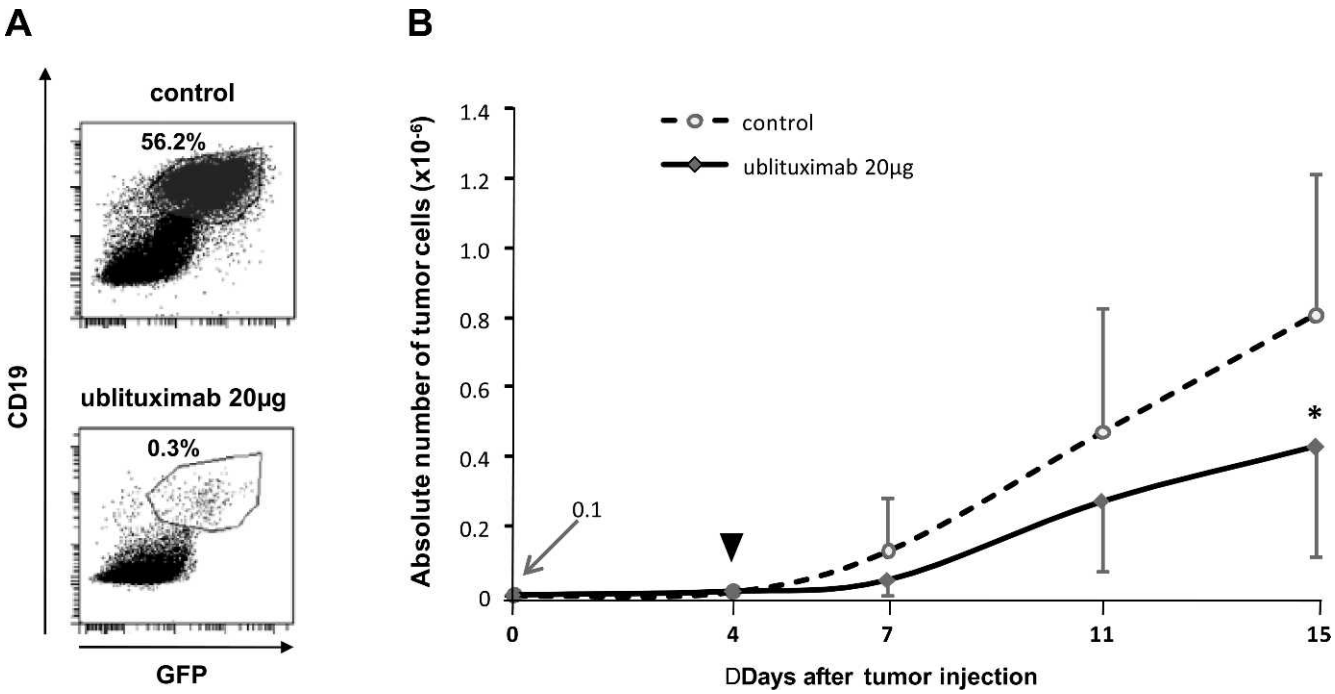

FIGURE 6. Analysis of the in vivo antitumor effect of anti-hCD20 ublituximab on PIOL. (**A**) Flow cytometric analysis on day 8 of PIOL eyes injected intravitreously in the tumor with 2 µL formulation buffer (control; *top panel*) or 2 µL containing 20 µg anti-hCD20 ublituximab (*lower panel*). (**B**) Kinetic analysis of the tumor burden by flow cytometry of PIOL eyes injected at day 4 in the tumor with 2 µL of formulation buffer (as control) or with 2 µL of anti-hCD20 ublituximab (20 µg).

unable to rescue mice implanted with the hCD20-negative tumor, but the survival time of mice with an hCD20-expressing tumor was greatly enhanced ($P < 0.0001$). Moreover, as previously observed, this treatment allowed 65% of the mice to reject their tumor. These results highlight the specificity against hCD20 of the antitumor response obtained after ublituximab therapy.

Anti-hCD20 Ublituximab Has a More Sustained and Better Antitumor Effect Than Rituximab on Primary Intraocular Lymphoma In Vivo

To determine if the anti-hCD20 ublituximab mAb had an antitumor effect on PIOL, immunocompetent BALB/c mice received an intravitreal injection of A20.IIA-GFP-hCD20 syngeneic lymphoma B cells 7 days before treatment. Mice were euthanized at different times following tumor implantation for ethical considerations related to the eye swelling. Clinically, as previously described,[15] vitreous and retinal invasion appeared at day 7 and increased progressively in control animals. However, vitreous haze or in some cases cataract after the second intraocular injection prevented clinical evaluation; the eyes were harvested for flow cytometric analyses (Fig. 6). Figure 6A illustrates the typical appearance of the tumor with and without anti-hCD20 therapy. The kinetics of tumor growth was also examined in mice that were or were not treated with 20 µg of ublituximab (Fig. 6B); tumor burden slowed after therapy, becoming significantly lower at day 15. Irrelevant glycoengineered mAbs of the same isotype as ublituximab were used as controls, and these groups (anti-D and anti-P24 mAbs) did not differ significantly from the PBS negative control group (Fig. 7).

A dose-response analysis was done with several concentrations of ublituximab (1, 4, and 20 µg/2 µL; Fig. 7). When ublituximab was injected at 4 µg/2 µL, the absolute number of tumor cells decreased significantly in comparison to the PBS 1X group ($P = 0.04$). In contrast, ublituximab injected at 1 µg/2 µL did not display significant efficacy.

Simultaneously, we sought to determine if the antitumor effect of ublituximab was superior to that of rituximab in the PIOL model, as it was in the PCL model, when these mAbs were administered at the same dose (20 µg/2 µL). Comparison of the absolute number of tumor cells 8 days after treatment showed it had decreased significantly in the ublituximab-

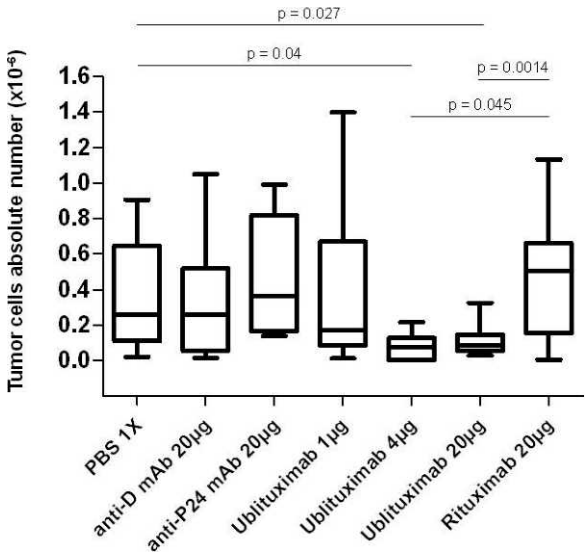

FIGURE 7. Analysis of the dose-response antitumor effect of anti-hCD20 ublituximab on PIOL. Tumor burden analysis by flow cytometry on day 8 of PIOL eyes injected at day 4 in the tumor with 2 µL of PBS (control group); anti-D mAb (20 µg); anti-P24 mAb (20 µg); rituximab (20 µg); or anti-hCD20 ublituximab (1, 4, or 20 µg). Statistical test: Mann-Whitney.

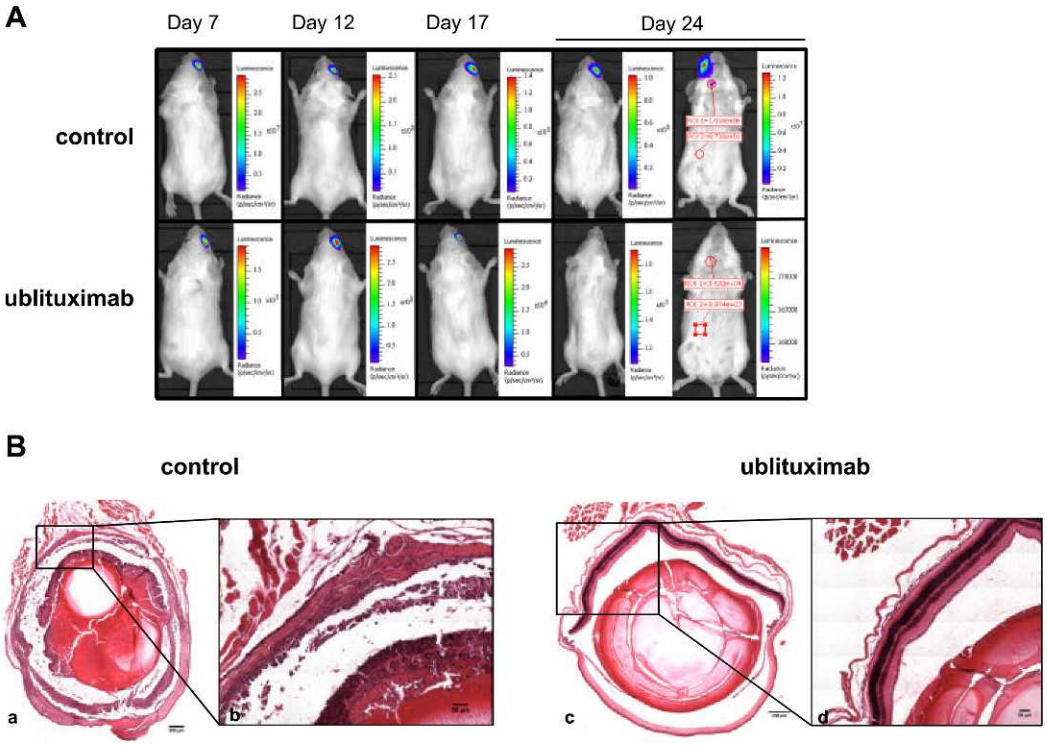

FIGURE 8. Representative bioluminescence images and histopathological analysis comparing ublituximab treatment with PBS injection in PIOL murine model. (**A**) Representative bioluminescence images of PBS control PIOL mice (*upper panel*) and ublituximab-treated PIOL mice (*lower panel*). The mice were injected with 10^4 A20.IIA-GFP-hCD20-luc2 cells on day 0 via the intravitreous route. The ublituximab treatments were administered in situ at day 7. (**B**) Representative histological aspect of PBS control PIOL mice (*left panels*) and ublituximab-treated PIOL mice (*right panels*). The mice were injected with 10^4 A20.IIA-GFP-hCD20-luc2 cells on day 0 via the intravitreal route. The ublituximab treatments were administered in situ at day 7 and sacrificed at day 21. (**a**, **c**) Magnification ×10 and *bars* represent 250 μm. (**b**, **d**) Magnification ×20 and *bars* represent 50 μm.

treated mice ($P = 0.027$) but not in those treated with rituximab (Fig. 7). The difference between the ublituximab and the rituximab-treated groups was highly significant ($P = 0.0014$) and confirmed the superiority of ublituximab in these conditions.

In bioluminescence assays, unlike in the PCL murine model, the effect of ublituximab in the PIOL model appeared later: a decrease of the tumor burden was visible at day 17 (i.e. 10 days after treatment; Fig. 8A). After 24 days, the representative PBS control mouse had a bioluminescence signal more than 200 times stronger than the ublituximab-treated mouse. In some cases (20%), histological analysis has revealed that no tumor mass could be detectable at day 21 in ublituximab-treated mice in contrast with control mice (Fig. 8B). Interestingly, some control mice had cervical lymph node metastasis, with 1×10^6 ph/s/cm^2/sr luminescence signal (Fig. 8A, RoI 1 in the upper panel), whereas the ublituximab-treated representative mouse had 2.6×10^4 ph/s/cm^2/sr in the right cervical lymph node (Fig. 8A, RoI 1 in the lower panel). Interestingly, anti-lymphoma antibodies were not detected in the control mice at day 19 (Supplementary Fig. 2B).

DISCUSSION

Most PCNSLs belong to the diffuse large B-cell lymphoma family. Although their incidence is low, it has nevertheless tripled over the past 10 years, for unknown reasons.[16] The main treatment against these tumors has been radiation coupled with chemotherapy.[17] As B-cell lymphomas express a well-characterized antigen, monoclonal antibodies are a promising therapy. Rituximab is a chimeric mAb directed against the human CD20 antigen shared by all B-cells, including B tumor cells. This antibody has shown its efficacy against systemic B-cell lymphomas,[18,19] and it has now been used for PCNSL.[20] In this study, we analyzed the efficacy of a glycoengineered anti-human CD20 monoclonal antibody developed by LFB for PIOL and PCL models and compared it with the efficacy of rituximab.

Until now, most preclinical evaluations of new therapies have used immunodeficient animals implanted with human tumors. These models are useful for assessing the direct efficacy of the treatment but cannot evaluate the immune system's influence on the therapeutic response. Syngeneic models can be useful for this purpose, but for an antigen-specific therapy, they must express the target antigen.[21] For this reason, we chose to work with two models based on the implantation of tumor cells transfected with the human CD20 gene, in the eye for the PIOL model[15,22] and in the brain for the PCL model[23] of adult syngeneic mice.

A significant increase in survival time without clinical signs was observed after a single injection of the new antibody into the brain of PCL-bearing mice, and half of the mice receiving the highest dose rejected their tumor. An interesting next step might be to multiply the number of therapeutic injections. However, repetitive injections into the brain are unlikely to be practical except if a delivery pump is implanted in the patient. Another possibility is to administer the therapeutic antibody intrathecally, which would allow its distribution throughout the entire CNS. This method has already been used clinically with rituximab with promising results,[24,25] and is currently under evaluation for ublituximab.

In our study and our conditions, rituximab was clearly less effective than ublituximab at the same therapeutic dose; only 10% of the rituximab-treated mice survived. The efficacy of rituximab against B-cell lymphoma in the brain has already been tested with the same general strategy we are using, and the authors reported a tumor rejection rate exceeding 50% after a single therapeutic injection of 25 μg.[4] However, they used a different mouse model and, more importantly, they applied the treatment very early (day 1) after tumor injection. This difference might explain the discrepancy with the results presented here.

Because we used immunocompetent mice, it was possible to determine the consequences of this therapy on the recruitment of effector immune cells. Our results clearly showed that after ublituximab therapy, $CD8^+$ T cells were recruited in the brain of PCL-bearing mice. These results are in line with recent studies showing that mAb therapy can create a memory response to a peripheral $CD20^+$ tumor[26] or to a subcutaneously implanted Neu^+ tumor.[27] This could be assessed in our model by rechallenging surviving mice with tumor cells.

It is interesting to note that results obtained on the PIOL model were less impressive. Tumor growth was delayed but not inhibited by the therapy with the optimized antibody. Eyes are often considered an extension of the CNS and they are thus thought to involve the same kind of immunoprivileged environment. Our results here suggest that eyes cannot respond as well as the brain to a B-cell lymphoma. One specific feature of the eye is its ability to suppress immune reactions even in inflammatory conditions.[28] More specifically, potential ocular antigen-presenting cells are maintained under a tolerogenic form, due to the high concentration of immunosuppressive factors in this site.[29] Ublituximab was developed to increase capacity to activate the ADCC pathway, compared with rituximab. It also induces the CDC pathway effectively. It is thus conceivable that the ocular environment decreases the capacity of the therapeutic antibodies to activate the ADCC effectively, whereas the brain environment is more permissive. Rituximab's lesser efficacy in inducing ADCC, compared with ublituximab, might also explain the difference in the results obtained with the two antibodies.

In this study, we demonstrated the efficacy of ublituximab in eliminating a B-cell lymphoma growing in two specific CNS locations, after a single therapeutic injection. Although the therapy did not cure all the animals, the results obtained in our study conditions were very encouraging and superior to those for rituximab, the reference mAb currently used. The new ublituximab mAb is thus a candidate for phase I/II studies of PIOL and PCL.

Acknowledgments

The authors thank the animal facility core (CEF, Centre de Recherche des Cordeliers, Paris, France) for mice housekeeping. Flow cytometry and acquisitions were done at the cellular imaging and cytometry platform (CICC, Centre de Recherche des Cordeliers, Paris, France). The authors thank Bernard Gjata, Thibaut Wiart, and Daniel Stockholm for their respective contribution to histological preparation and image acquisitions (histology and imaging cytometry platforms, Généthon, Evry, France). We thank Peter Sportelli for allowing the use of ublituximab, and Jo Ann Cahn for her careful reading of the manuscript.

Supported by the Institut National du Cancer (Grants RC013-C06N631-2005 and C06N748-2006); the Association pour la Recherche contre le Cancer; the Institut National de la Santé et de la Recherche Médicale; the University Pierre and Marie Curie; the University Paris-Descartes; the pole de compétitivité Ile de France (ImmuCan project); the Tunisian Direction Générale de la Recherche Scientifique; the Franco-Tunisian CMCU project; grants from the DGRS-INSERM and the CMCU (RBA); a grant from the Institut National du Cancer (SD, CD); and study grants from the Fédération des Aveugles de France and the Fondation de France (Fouassier; VT). The authors alone are responsible for the content and writing of the paper.

Disclosure: **R. Ben Abdelwahed**, LFB (F); **S. Donnou**, LFB (F); **H. Ouakrim**, LFB (F); **L. Crozet**, LFB (F); **J. Cosette**, LFB (F); **A. Jacquet**, LFB (F, E); **I. Tourais**, LFB (F, E); **B. Fournès**, LFB (F, E); **M. Gillard Bocquet**, LFB (F); **A. Miloudi**, LFB (F); **V. Touitou**, LFB (F); **C. Daussy**, LFB (F); **M-C. Naud**, LFB (F); **W.H. Fridman**, LFB (F); **C. Sautès-Fridman**, LFB (F), P; **R. Urbain**, LFB (F, E), P; **S. Fisson**, LFB (F), P

References

1. Miller DC, Hochberg FH, Harris NL, Gruber ML, Louis DN, Cohen H. Pathology with clinical correlations of primary central nervous system non-Hodgkin's lymphoma. The Massachusetts General Hospital experience 1958–1989. *Cancer*. 1994;74:1383–1397.
2. Algazi AP, Kadoch C, Rubenstein JL. Biology and treatment of primary central nervous system lymphoma. *Neurotherapeutics*. 2009;6:587–597.
3. Soussain C, Hoang-Xuan K. Primary central nervous system lymphoma: an update. *Curr Opin Oncol*. 2009;21:550–558.
4. Mineo JF, Scheffer A, Karkoutly C, et al. Using human CD20-transfected murine lymphomatous B cells to evaluate the efficacy of intravitreal and intracerebral rituximab injections in mice. *Invest Ophthalmol Vis Sci*. 2008;49:4738–4745.
5. Rosenzweig HL, Planck SR, Rosenbaum JT. NLRs in immune privileged sites. *Curr Opin Pharmacol*. 2011;11:423–428.
6. Hong SJ, Kim JS, Chang JH, et al. A successful treatment of relapsed primary CNS lymphoma patient with intraventricular rituximab followed by high-dose chemotherapy with autologous stem cell rescue. *Yonsei Med J*. 2009;50:280–283.
7. Motomura K, Natsume A, Fujii M, Ito M, Momota H, Wakabayashi T. Long-term survival in patients with newly diagnosed primary central nervous system lymphoma treated with dexamethasone, etoposide, ifosfamide and carboplatin chemotherapy and whole-brain radiation therapy. *Leuk Lymphoma*. 2011;52:2069–2075.
8. Amadori D, Milandri C, Comella G, et al. A phase I/II trial of non-pegylated liposomal doxorubicin, docetaxel and trastuzumab as first-line treatment in HER-2-positive locally advanced or metastatic breast cancer. *Eur J Cancer*. 2011;47:2091–2098.
9. van Oers MH, Van Glabbeke M, Giurgea L, et al. Rituximab maintenance treatment of relapsed/resistant follicular non-Hodgkin's lymphoma: long-term outcome of the EORTC 20981 phase III randomized intergroup study. *J Clin Oncol*. 2010;28:2853–2858.
10. Jahnke K, Thiel E. Treatment options for central nervous system lymphomas in immunocompetent patients. *Expert Rev Neurother*. 2009;9:1497–1509.
11. van Beek J, Elward K, Gasque P. Activation of complement in the central nervous system: roles in neurodegeneration and neuroprotection. *Ann N Y Acad Sci*. 2003;992:56–71.
12. de Romeuf C, Dutertre CA, Le Garff-Tavernier M, et al. Chronic lymphocytic leukaemia cells are efficiently killed by an anti-CD20 monoclonal antibody selected for improved engagement of FcgammaRIIIA/CD16. *Br J Haematol*. 2008;140:635–643.
13. Le Garff-Tavernier M, Decocq J, de Romeuf C, et al. Analysis of CD16+CD56dim NK cells from CLL patients: evidence supporting a therapeutic strategy with optimized anti-CD20 monoclonal antibodies. *Leukemia*. 2011;25:101–109.

14. Jones B, Tite JP, Janeway CA Jr. Different phenotypic variants of the mouse B cell tumor A20/2J are selected by antigen- and mitogen-triggered cytotoxicity of L3T4-positive, I-A-restricted T cell clones. *J Immunol*. 1986;136:348–356.
15. Touitou V, Daussy C, Bodaghi B, et al. Impaired th1/tc1 cytokine production of tumor-infiltrating lymphocytes in a model of primary intraocular B-cell lymphoma. *Invest Ophthalmol Vis Sci*. 2007;48:3223–3229.
16. Gerstner ER, Batchelor TT. Imaging and response criteria in gliomas. *Curr Opin Oncol*. 2010;22:598–603.
17. Ferreri AJ. How I treat primary CNS lymphoma. *Blood*. 2011; 118:510–522.
18. Molina A. A decade of rituximab: improving survival outcomes in non-Hodgkin's lymphoma. *Annu Rev Med*. 2008;59:237–250.
19. Niitsu N. Current treatment strategy of diffuse large B-cell lymphomas. *Int J Hematol*. 2010;92:231–237.
20. Tai WM, Chung J, Tang PL, et al. Central nervous system (CNS) relapse in diffuse large B cell lymphoma (DLBCL): pre- and post-rituximab. *Ann Hematol*. 2011;90:809–818.
21. Donnou S, Galand C, Touitou V, Sautes-Fridman C, Fabry Z, Fisson S. Murine models of B-cell lymphomas: promising tools for designing cancer therapies. *Adv Hematol*. 2012;2012: 701704.
22. Touitou V, Bodaghi B, de Kozak Y, Lehoang P, Sautes-Fridman C, Fisson S. Animal models of intraocular lymphomas. *Ophthalmic Res*. 2008;40:208–211.
23. Donnou S, Galand C, Daussy C, et al. Immune adaptive microenvironment profiles in intracerebral and intrasplenic lymphomas share common characteristics. *Clin Exp Immunol*. 2011;165:329–337.
24. Maximiano Alonso C, Sanchez Ruiz AC, Cantos Sanchez de Ibarguen B, Mendez Garcia M, Ronco IS, Provencio Pulla M. Ocular relapse of primary brain lymphoma in immunocompetent patient, treated with intrathecal rituximab. *Clin Transl Oncol*. 2010;12:701–703.
25. Rubenstein JL, Fridlyand J, Abrey L, et al. Phase I study of intraventricular administration of rituximab in patients with recurrent CNS and intraocular lymphoma. *J Clin Oncol*. 2007; 25:1350–1356.
26. Abes R, Gelize E, Fridman WH, Teillaud JL. Long-lasting antitumor protection by anti-CD20 antibody through cellular immune response. *Blood*. 2010;116:926–934.
27. Park S, Jiang Z, Mortenson ED, et al. The therapeutic effect of anti-HER2/neu antibody depends on both innate and adaptive immunity. *Cancer Cell*. 2010;18:160–170.
28. Mo JS, Wang W, Kaplan HJ. Impact of inflammation on ocular immune privilege. *Chem Immunol Allergy*. 2007;92:155–165.
29. Wilbanks GA, Streilein JW. Fluids from immune privileged sites endow macrophages with the capacity to induce antigen-specific immune deviation via a mechanism involving transforming growth factor-beta. *Eur J Immunol*. 1992;22:1031–1036.

Investigative Ophthalmology & Visual Science